NeuroImage **13,** 283–294 (2001)
doi:10.1006/nimg.2000.0698, available online at http://www.idealibrary.com on IDEAL®

Three-Dimensional Electrical Impedance Tomography of Human Brain Activity

Tom Tidswell, Adam Gibson, Richard H. Bayford,* and David S. Holder

*Department of Clinical Neurophysiology, Middlesex Hospital, University College London, London W1N 8AA, United Kingdom; and *School of Health, Environment and Biological Sciences, Middlesex University, Archway Campus, London N19 5ND, United Kingdom*

Received June 30, 2000

Regional cerebral blood flow and blood volume changes that occur during human brain activity will change the local impedance of that cortical area, as blood has a lower impedance than that of brain. Theoretically, such impedance changes could be measured from scalp electrodes and reconstructed into images of the internal impedance of the head. Electrical Impedance Tomography (EIT) is a newly developed technique by which impedance measurements from the surface of an object are reconstructed into impedance images. It is fast, portable, inexpensive, and noninvasive, but has a relatively low spatial resolution. EIT images were recorded with scalp electrodes and an EIT system, specially optimized for recording brain function, in 39 adult human subjects during visual, somatosensory, or motor activity. Reproducible impedance changes of about 0.5% occurred in 51/52 recordings, which lasted from 6 s after the stimulus onset to 41 s after stimulus cessation. When these changes were reconstructed into impedance images, using a novel 3-D reconstruction algorithm, 19 data sets demonstrated significant impedance changes in the appropriate cortical region. This demonstrates, for the first time, that significant impedance changes, which could form the basis for a novel neuroimaging technology, may be recorded in human subjects with scalp electrodes. The final images contained spatial noise and strategies to reduce this in future work are presented.

INTRODUCTION

Electrical impedance tomography (EIT) is a relatively new, portable, medical imaging technique with which impedance images of an object are reconstructed from measurements made at electrodes on the surface of the object. Each impedance measurement is made from a combination of four electrodes: two apply an alternating current which produces a voltage field on the surface of the object, and this voltage field is measured between different pairs of electrodes. The boundary impedance is then calculated from the known voltage and applied current. The current and voltage electrodes are switched through different combinations of electrodes so that the transfer impedance is measured for different positions of the applied current. These measurements may be related to the internal impedance of the object, by means of a reconstruction algorithm calculated from a model of the object, and so an impedance image of the object can be reconstructed (Brown and Seagar, 1987). EIT has been used in humans to image impedance changes in the chest produced during ventilation and the cardiac cycle (Metherall *et al.*, 1996) and in the abdomen during gastric emptying (Mangall *et al.*, 1987). We present the first data collected with EIT from scalp electrodes during functional activity in humans. In this work, EIT was used to image impedance differences between a baseline and stimulation condition. This approach minimises errors due to the instrumentation, and a mismatch between the model used to derive the reconstruction algorithm and the actual measurement conditions.

The electrical impedance of brain is determined by the relative volumes and differing impedances of the neurones, glial cells, blood, and extra-cellular fluid. Changes to the relative volume of these components will affect brain impedance. For example, an increase of regional cerebral blood volume (rCBV), as a result of neuronal activity, will decrease cortical impedance because blood has a lower impedance than the surrounding cortex (Ranck, 1963; Geddes and Baker, 1967). If such changes can be measured, then EIT could be used to image brain activity. Evidence that cortical impedance changes during functional activity and epilepsy has been demonstrated in studies that used intracortical electrodes in cats and rabbits (Adey *et al.*, 1962; Van-Harreveld and Schade, 1962; Aladjolova, 1964). There are two possible opposing changes that would dominate the impedance change. During functional activity, there is a predominant impedance decrease, due to an increase in blood volume. During epilepsy and ischaemia, impedance increases due to cell swelling, as

1053-8119/01 $35.00

this reduces the size of the conductive extra-cellular space (Lux *et al.,* 1986; Andrew and Mac Vicar, 1994). Similar impedance changes have recently been imaged with EIT in rabbits during sensory evoked responses (Holder *et al.,* 1996) and epilepsy (Rao, 2000). In both studies measurements were made with a ring of electrodes placed on the exposed cortex. The peak impedance changes in the images were localised to the visual cortical area during strobe light stimulation, the contralateral somatosensory cortex during forepaw stimulation, and to the focus of the electrical stimulus which produced epilepsy. Impedance decreases of about 5% were measured during functional activity and increases of 10% during epilepsy. The impedance increase during epilepsy was partly opposed by a 0.4% impedance decrease produced by a 0.3°C rise of cortical temperature. Such temperature increases affect ionic conductivity due to increased ionic movements (Van-Harreveld and Ochs, 1956). However, during epilepsy, temperature only had a small effect on the overall impedance change.

Brain activity in humans should produce similar impedance changes, as brain activity produces changes in regional cerebral blood flow (rCBF), measured with Positron Emission Tomography (PET) (Mazziotta and Phelps, 1984; Fox *et al.,* 1986) and functional magnetic resonance imaging (fMRI) (Belliveau *et al.,* 1991; Kwong *et al.,* 1992). These blood flow changes, which are usually increases, are associated with increased rCBV. This has been demonstrated by optical imaging of evoked brain activity in animals (Malonek *et al.,* 1997; Palmer *et al.,* 1999) and human studies (Haglund *et al.,* 1992). Small impedance changes may also be produced by changes of cortical temperature (Yablonskiy *et al.,* 2000). In an fMRI study of visual stimulation a cooling effect of 0.2°C in the activated visual cortex was estimated to be due to increased rCBF. The likely mechanism is that there is increased flow of blood at body temperature, which is cooler than that of the metabolically active cortex. However, although this would increase cortical impedance by approximately 0.4% (Van-Harreveld and Ochs, 1956), this change is likely to be dominated by the 5% impedance decreases expected from increased rCBV (Holder *et al.,* 1996).

The combined cerebral impedance changes produced by changes in rCBV and temperature could be imaged with EIT, provided that the impedance signal from the brain is not attenuated beyond the sensitivity of the EIT system by the presence of the skull. The skull acts as a high impedance barrier to current flow, so that a large proportion of current will pass through the path of least resistance within the scalp and a smaller proportion of the applied current will enter the brain. The presence of the skull is expected to attenuate the measured impedance change by a factor of perhaps five (Gibson *et al.,* 2000; Joy *et al.,* 1999) and distort the EIT images so that impedance changes are imaged more centrally than their true position, if the model for the reconstruction algorithm is a homogeneous sphere (Avis *et al.,* 1992; Tidswell *et al.,* 2000).

In this paper, images of the internal impedance change of the head were reconstructed from the scalp impedance changes. This involved two steps. First, a "sensitivity matrix," which describes how the boundary impedance of a sphere should change with changes in its internal impedance, was calculated analytically by assuming the head to be a homogeneous sphere. Then this matrix was inverted by singular value decomposition. Images were produced by multiplying the scalp impedance changes by the inverted sensitivity matrix (Gibson, 2000).

The purpose of this study was to extend the previous animal work and determine whether EIT could detect impedance changes during functional brain activity in humans using scalp electrodes. A secondary purpose was to calibrate a new 3-D EIT system and reconstruction algorithm optimized for the head. If human-evoked responses can be imaged, then EIT could be used to image the larger impedance changes due to cell swelling that occur during epilepsy, spreading depression (Boone *et al.,* 1994) and cortical ischaemia (Holder, 1992). EIT at present has a relatively low spatial resolution: for example the full width at half maximum (FWHM) was 25% of the image diameter using a 31 electrode EIT system, developed in our group, and used on a realistic head model which incorporated a human skull (Tidswell *et al.,* 2000; Fig. 2). In future it is likely that the spatial resolution will improve, with larger number of electrodes and improved reconstruction algorithms. It could offer a significant advance in the field of neuroimaging as it would be a low cost, portable, and fast imaging system capable of imaging epilepsy, migraine, and stroke. In addition, EIT could also be used in conjunction with EEG, for the telemetry and localization of epilepsy prior to neurosurgery (Holder *et al.,* 1994; Rao, 2000).

MATERIALS AND METHODS

Overview

EIT measurements were made with scalp electrodes, during visual, sensory, or motor stimulation in adult volunteers. An EIT image data set was acquired every 25 s throughout an experiment lasting 6 min, 15 s. Experiments were repeated 6–12 times in each subject to allow averaging. Both the scalp impedance data and the reconstructed images were analysed for reproducible changes. As the images were reconstructed using a new 3-D reconstruction algorithm optimised for the head, the EIT system and algorithm were also calibrated by imaging objects inside a human skull within a saline filled head-shaped tank.

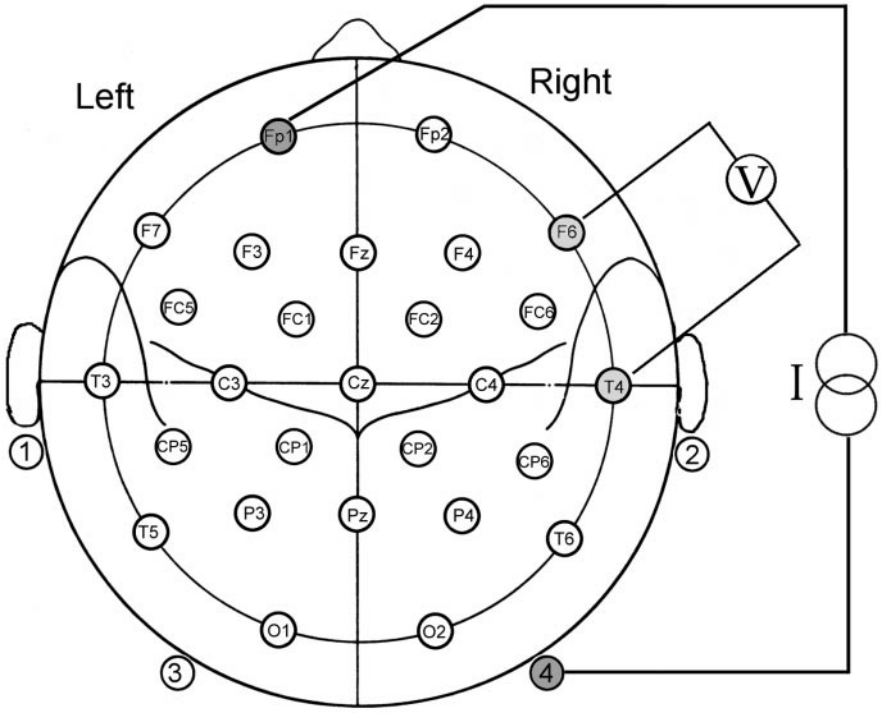

FIG. 1. EIT electrode positions, viewed from above the head. Those taken from the International 10-20 system are labeled according to that system. Four modified positions were also used; electrodes 1 and 2 were placed on the mastoid bones behind each ear and electrodes 3 and 4 placed over the base of the occiput. A single impedance measurement is represented in this diagram: a 50 kHz alternating current, **I,** was applied through electrodes Fp1 and 4, and the voltage, **V,** measured from electrodes F6 and T4. In total 258 impedance measurements were made at different electrode combinations for each EIT image.

Subjects

Measurements were made in 39 healthy adults (mean age 42 years, range 16–64) who had no neurological problems and had given informed consent to the study. The subjects were seated in a reclined chair in a quiet and darkened room: 26 subjects took part in one experimental paradigm and 13 in two stimulation paradigms, a total of 52 recordings.

Experimental Paradigms

Stimuli were (1) Visual: observation of a 0.6° checkerboard oscillating at 8 Hz (n = 14 experiments) on a black and white monitor placed 70 cm in front of the subject; (2) Motor: self paced, sequential apposition of the thumb and fingers (n = 20 experiments, 13 right hand, 7 left hand); or (3) Somatosensory: electrical stimulation of the median nerve at the wrist with a 3 Hz, 0.1 ms square wave pulse at a threshold required to produce a thumb twitch (n = 18 experiments, 10 right, 8 left). Each stimulus was presented for 75 s during a 6 min, 15 s experiment. A long stimulation paradigm was used, due to the relatively slow image acquisition time of 25 s. This allowed 15 EIT image data sets to be acquired, sufficient for the correction of baseline drift and analysis of the timecourse of the impedance response. Baseline conditions before and after the stimulus were darkness for the visual paradigms or sitting still with eyes closed for the motor and somatosensory paradigms. Impedance measurements obtained during stimulation were compared to baseline impedance measurements in order to determine the impedance change due to brain activity.

EIT Acquisition

Thirty-one silver/silver-chloride EEG cup electrodes were applied to the head in a modified 10–20 system of electrode placement (Binnie *et al.*, 1982; Fig. 1). Impedance measurements were made with an HP 4284A impedance analyzer (Hewlett Packard, http://www.hewlettpackard.com), modified to allow the four terminals of the impedance analyser to be switched through different combinations of the scalp electrodes (Gersing, 1991; Bayford *et al.*, 1996); two terminals applied a current between 1 and 2.5 mA at 50 kHz, and two terminals recorded voltage. The current electrodes were selected to be diametrically opposed to each other across the head in order to maximise the sensitivity of the EIT system to brain impedance changes (Tarassenko *et al.*, 1985; Bayford *et al.*, 1996). Each image comprised 258 independent impedance measurements made over 25 s; 15 images were acquired per experiment, and each such experiment was repeated at least

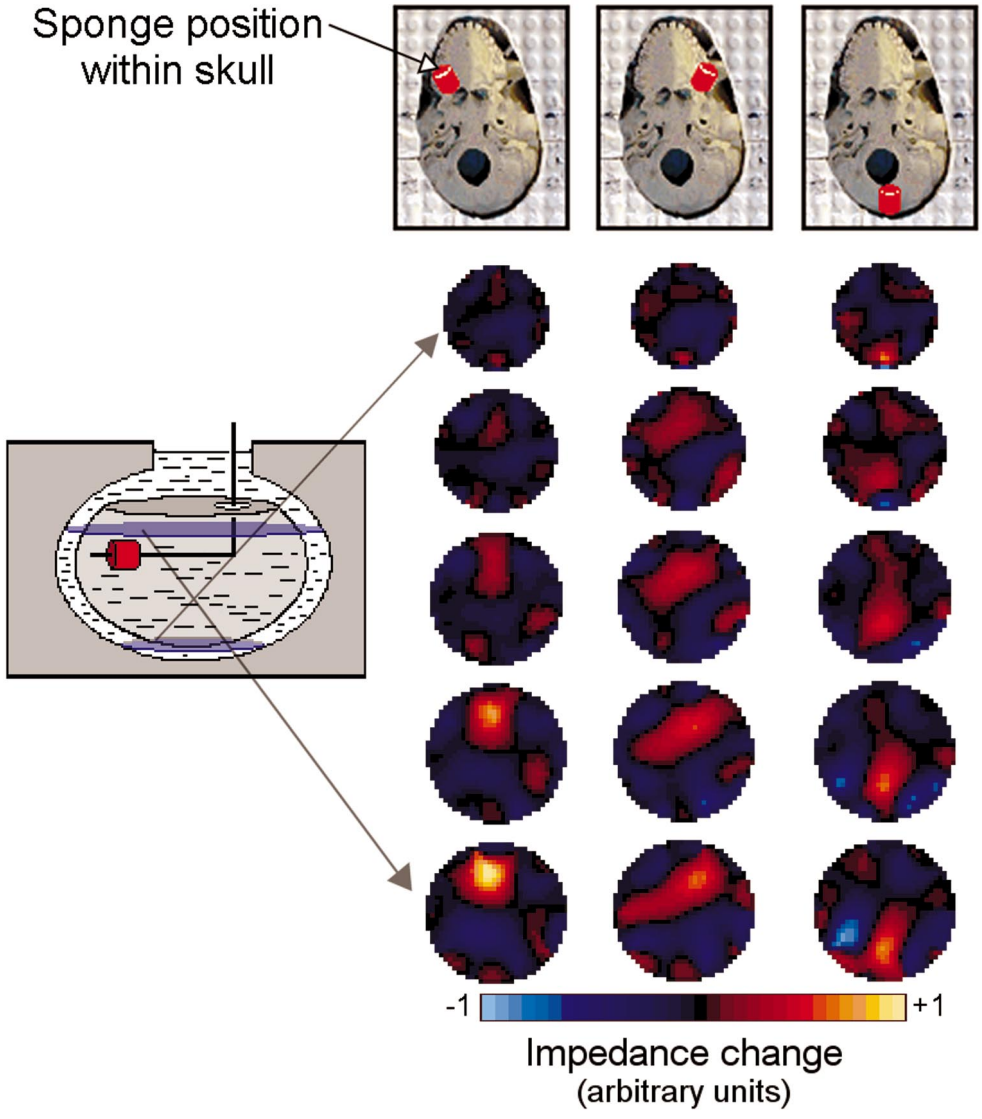

FIG. 2. Calibration of the EIT system by imaging a sponge inside a human skull in a saline-filled head-shaped tank. The tank (left) had 31 electrodes on its inner surface through which impedance measurements were made. A sponge, inserted through the foramen magnum on a wooden support, was imaged in three positions. The size of the sponge in relation to the tank was 14 and 16% of the tank length and width, respectively. Each image is represented by a column of five transverse slices through the tank, the sponge position is indicated at the top of the corresponding images. The impedance increases due to the sponge, seen in red, are localized to within 12% of the image diameter of their actual positions in the tank. The FWHM of the imaged sponge was 25% of the image diameter. The impedance decreases, seen in blue, do not correspond to an impedance change in the tank and are artefactual in origin.

six times for each stimulation paradigm per subject. The 258 measurements per image represented a subset of the 419 possible independent measurements available from 31 scalp electrodes, given the constraint of diametric current application. This subset was selected in order to reduce the image acquisition time to a period suitable for human imaging.

The acquired data was analysed and corrected for baseline drift and excess noise by programs written in Matlab (Mathworks Inc., http://www.mathworks.com). As the impedance of the electrode-skin interface drifts approximately linearly over the duration of an experiment (Boone and Holder, 1995), the data was corrected at each electrode measurement by the subtraction of a line made from a least squares fit to the baseline data. The data was then expressed as a percentage change from the mean baseline impedance. Electrode measurements were then eliminated if the baseline noise or movement artefact exceeded 1% of the baseline impedance. An experiment was rejected from subsequent analysis if 25% or more electrode measurements were eliminated for noise.

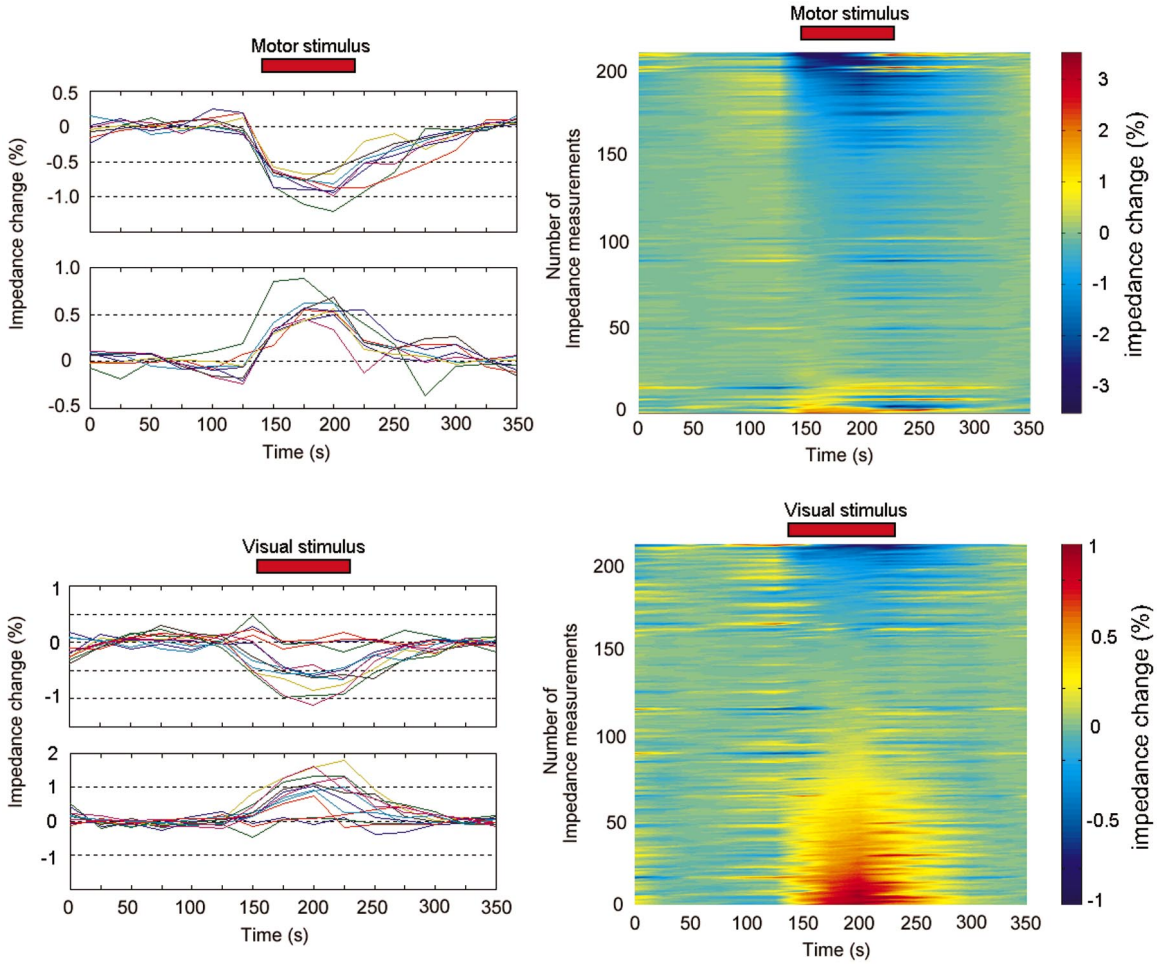

FIG. 3. Impedance changes, prior to image reconstruction, from a subject who performed hand motor activity (top row, $n = 8$ experiments) and a subject during visual stimulation (bottom row, $n = 12$). On the left, data are shown from single selected electrode combinations, with data from all experiment runs superimposed. Reproducible impedance changes are seen at selected electrode combinations with the same timecourse as the stimulation paradigms. The y-axis indicates the percentage change from baseline impedance. Impedance measurements were made every 25 s; the lines between these measurements are drawn for clarity. Both impedance increases and decreases were observed. On the right are shown data for the same subjects. The 8–12 runs for each electrode combination were averaged together. For clarity the resulting 258 data sets were sorted due to the size of the impedance change during stimulation and stacked on the vertical axis. Measurements with baseline noise greater than the impedance changes are excluded from these plots so that these changes are not obscured. Stimulus related impedance increases and decreases are seen in approximately 25% of electrode measurements in these subjects.

Image Reconstruction

The reconstructed EIT images represent a spatially smoothed and low resolution image of the impedance changes within the head, in which the pixels are inversely related to the conductivity changes, $\Delta\boldsymbol{\sigma}$. These conductivity changes are related to voltage changes measured at the scalp, $\Delta\mathbf{V}$, when a current is applied to the head. This relationship is expressed in matrix form by Poisson's equation:

$$\Delta\mathbf{V} = \mathbf{A}\Delta\boldsymbol{\sigma},$$

where $\mathbf{A}$ is known as the sensitivity matrix. The problem is to solve the equation to find $\Delta\boldsymbol{\sigma}$, given the measured voltages, $\Delta\mathbf{V}$, which are proportional to the boundary impedance measurements. This was done by calculating the sensitivity matrix analytically for a model of the head as a sphere of uniform conductivity. The matrix was then inverted, by truncated singular value decomposition (SVD), in which the sensitivity matrix was decomposed into a series of orthogonal matrices, each associated with a weighting factor—a singular value (Golub and Loan, 1996). However, as errors in the sensitivity matrix are emphasised by the inversion process and can severely distort the final images, these errors are suppressed by truncating the inversion process at a point before noise is introduced into the images. This threshold depends on the size of noise in the impedance data, the size of the errors in the sensitivity matrix and the numerical rank of the

TABLE 1

Summary of the Raw Impedance Data—Size and Number of Stimulus-Related Impedance Changes

Stimulation paradigm (number of subjects)	Average number of electrode combinations with stimulus-related impedance change (% of total)	Average impedance change (% of baseline impedance)
Visual ($n = 13$)	25 ± 3%	0.43 ± 0.05%
Motor ($n = 20$)	26 ± 3%	0.34 ± 0.05%
Somatosensory ($n = 18$)	12 ± 2%	0.19 ± 0.02%

Note. All data is presented as mean ± SE.

sensitivity matrix, determined by the number of independent impedance measurements (Gibson, 2000; Breckon, 1990). For the human data, the number of independent measurements was determined by SVD. Of 258 electrode combinations used in this study, 255 appeared independent (Gibson, 2000). However, a truncation threshold of 62 singular values was chosen, as this was appropriate for the level of noise present in the impedance data.

Once the inverted sensitivity matrix, $\mathbf{A}^{-1}$ is calculated, Poisson's equation can be rewritten:

$$\Delta\boldsymbol{\sigma} = \mathbf{A}^{-1}\Delta\mathbf{V},$$

from which the image of impedance change in the head can be calculated for any set of measured voltage changes.

Calibration of the EIT System

The reconstruction algorithm was validated on EIT data collected from a realistically head shaped, 0.2% saline-filled tank that contained a human skull and electrodes in identical positions to those used on the human volunteers. A 12% impedance increase, similar to the change produced by epilepsy in rabbits, was produced by a polyurethane sponge (Vitafoam, UK), density 5% w/v, 2.5 cm diameter, and 2.8 cm length, inserted inside the saline-filled skull. The images obtained localised the sponge to within 12% of the image diameter of its true position in the tank. The FWHM of the sponge was 25% of the image diameter (Fig. 2). To determine whether noise correction of the human data had an effect on image localization of an impedance change, images of the sponge were produced with successive amounts of simulated noise correction on the data. Up to 40% of electrode measurements could be eliminated without a noticeable effect on the localization of the sponge, although the magnitude of the imaged change was reduced. These results indicate that the positional information in the EIT images is contained within a subset of the impedance measurements, and suggest that the elimination of 2–25% of the human electrode measurements, due to noise, will not significantly affect image localization.

Image Analysis

Images produced were difference images between the stimulus and baseline conditions. The images were averaged across trials for each subject. A significant impedance change was defined as a change with the same timecourse as the stimulus, that had a FWHM of 25% of the image diameter or more and the pixels within the FWHM were more than 2 standard errors of the mean from baseline. This size of FWHM was chosen because it was the minimum FWHM of an object imaged within the head shaped tank, used to calibrate the EIT system and algorithm. Some of the images acquired immediately after stimulus onset were affected by the latency of the impedance response. This meant that early measurements within a few seconds of stimulus onset did not measure an impedance change whereas data acquired later in that image did. This had the effect of reducing the size, but not the location, of an impedance change in the image acquired immediately after the stimulus onset. If this image did not meet the criteria of a significant change but subsequent stimulus images did, then this was considered to be a significant stimulus related change.

The appropriate localization of a significant impedance change was defined for each stimulus modality from the results of rCBV changes measured in functional imaging studies, from the literature, which have used either PET or fMRI. These were: (1) The posterior quadrant of the EIT images, which corresponded to the visual cortex (Fox *et al.,* 1986), or (2) The contralateral image quadrants to the moving or stimulated hand that corresponded to the contralateral motor (Kim *et al.,* 1993) or somatosensory cortex (Ibanez *et al.,* 1995), respectively. As the EIT images did not contain anatomical information to allow coregistration with a standard anatomical template, then the image orientation was defined from the position of the scalp electrodes and the corresponding electrode positions in the reconstruction model. Although there may be small errors in orientation due to errors in electrode positioning, these are likely to be small in comparison to the FWHM of an imaged impedance change and are unlikely to have a noticeable effect on impedance change localization.

RESULTS

Raw Data

Reproducible impedance increases and decreases with a time course similar to the stimulus period were observed in 51/52 recordings (Table 1). One visual recording was rejected from further analysis due to excess noise from movement artifact. Significant impedance changes were defined as those more than 2 standard errors of the mean (SEM) from the baseline impedance in two or more consecutive stimulus frames. Such significant impedance changes were seen in 25 ± 3% (n = 13, mean ± SEM), 26 ± 3% (n = 20), and 12 ± 2% (n = 18) of the electrode combinations in each subject for visual, motor, and somatosensory paradigms, respectively. Both impedance increases and decreases were seen (Fig. 3). The absolute mean impedance change, averaged over electrodes with a significant change during the stimulation period, was significantly lower in the somatosensory experiments (0.19 ± 0.02%) compared to both the visual (0.43 ± 0.05%) and motor (0.34 ± 0.05%) experiments ($P <$ 0.01, 2-tailed t test). There was no significant difference between the mean signal of the visual and motor groups. The timecourse of the impedance change was calculated for the motor activation experiments: impedance changed 5.8 ± 0.9 s after stimulus onset and returned to within 2 SEM of the baseline 41.3 ± 2.4 s after stimulus cessation.

To examine the possibility that the impedance changes had arisen from changes in the scalp tissues, further experiments were performed in 5 additional subjects. Impedance data were obtained, as described above for the imaging experiments, during a right hand motor paradigm. The data were immediately analysed and an electrode combination selected that demonstrated a significant impedance change. The four EEG electrodes used to make this measurement were replaced with four electrode arrays, each of which consisted of 4 electrodes spaced 4 mm apart. These were designed to be sensitive to impedance changes in the scalp directly beneath the electrode array. Scalp impedance was then recorded during repetition of the motor task. Scalp impedance did not change from baseline noise during motor activity (0.04 ± 0.01% vs 0.08 ± 0.02%, P = 0.36, t test), whereas the impedance change measured during image acquisition was significantly greater than baseline noise (0.42 ± 0.04% vs 0.12 ± 0.02%, $P <$ 0.00005, t test).

Image Analysis

On reconstruction, significant changes, as defined above, were imaged in the appropriate area of the brain for the visual, motor, and somatosensory cortices, respectively, in 9/13 visual, 8/20 motor, and 2/18 somatosensory subjects (Figs. 4 and 5). Images with a significant impedance change but in the incorrect location were found in 4/13 visual, 9/20 motor, and 5/18 somatosensory experiments (Table 2).

DISCUSSION

To our knowledge, this is the first time that impedance changes associated with physiological evoked responses have been measured noninvasively in humans. Images of these changes have been reconstructed by the first 3-D EIT reconstruction algorithm, which has been optimised for the head and validated on data acquired from a head shaped tank (Gibson, 2000). Significant impedance changes were measured in nearly all the subjects during visual, motor, or somatosensory stimulation. As these changes did not occur at the scalp, it is likely that the origin of these evoked impedance changes was from the brain. It is possible that there were also contributions from impedance changes in the surrounding CSF and penetrating blood vessels. However, these impedance changes are consistent with the hypothesis that changes in rCBV, due to stimulated neural activity, change brain impedance.

Unfortunately, the EIT images did not demonstrate consistent localisation of the impedance changes to the area expected from the stimulation paradigms. The failure to demonstrate any significant impedance changes in an individual image was related to a significantly lower signal to noise ratio (SNR) present in the raw impedance data: for images without a significant change the SNR was 0.76 ± 0.36 (n = 14, mean ± SD) compared to 1.34 ± 0.63 (n = 37) for images with significant changes ($P <$ 0.01, 2 tailed t test). The majority of the images without a significant change were from the somatosensory group, which also had a smaller average signal than either the visual or motor responses. The low signal present in some subjects may be due to small changes of rCBV. This is supported by a study (Kinahan and Noll, 1999) in which 2/7 subjects showed no blood flow changes detectable with either PET or fMRI during hand motor activity.

However, in 18/51 subjects, significant impedance changes were seen in areas away from the expected site of cortical stimulation. If these changes were produced by impedance changes in the expected site of cortical activity, then these images demonstrate errors of localisation. Such errors may be produced by either the inaccurate modelling of the head as a homogenous sphere in the reconstruction algorithm, errors of electrode positioning, image distortion due to the layered structure of the head or reconstruction artefacts. Electrode positioning errors were minimized by the use of a standardised system of electrode placement. The estimated placement errors were 1 cm, which is approximately 2% of the head circumference. As similar electrode positioning errors existed in the head-tank, which did not cause large localisation errors, it is un-

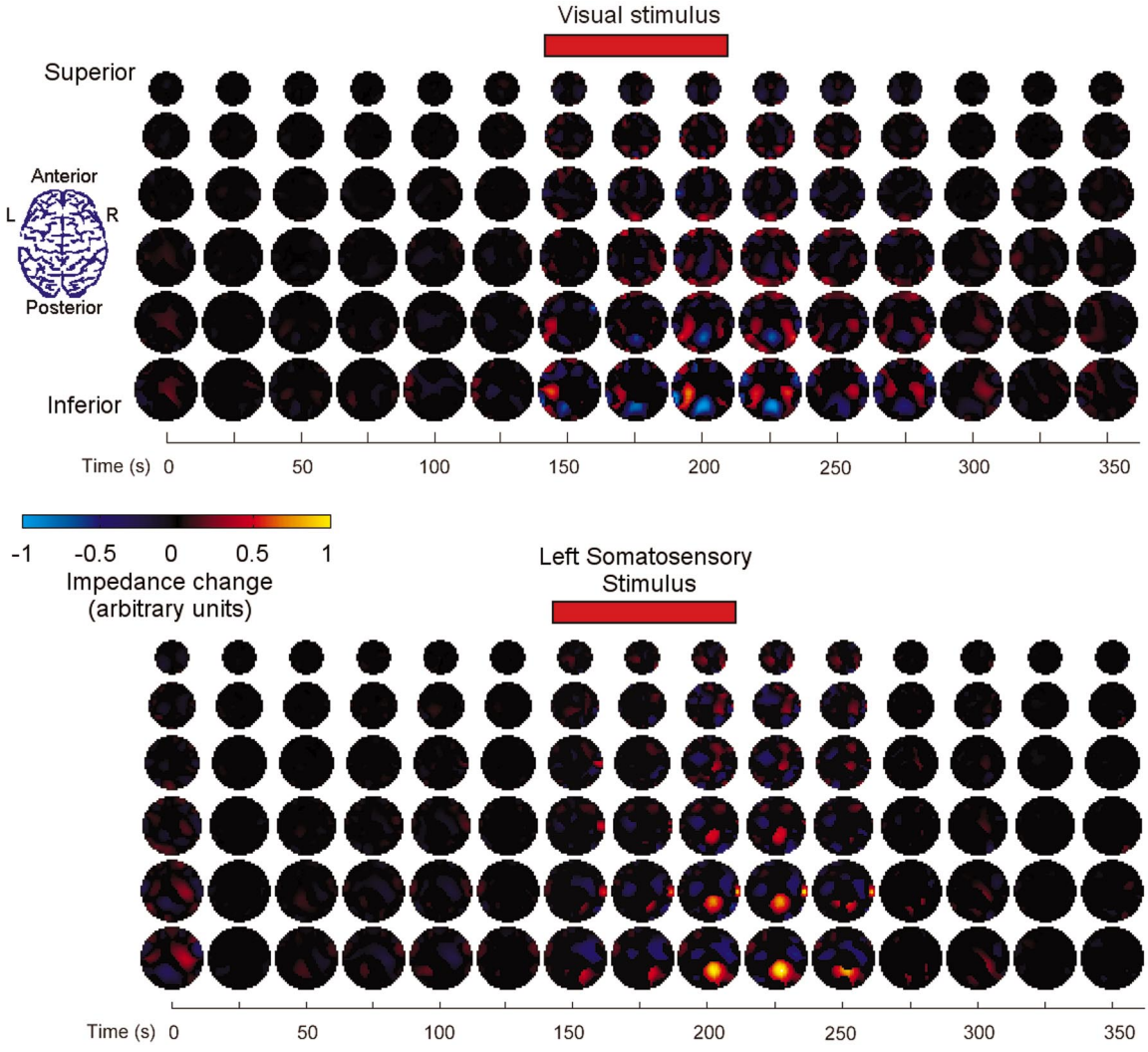

FIG. 4. Impedance images in subjects during (top) visual stimulation (averaged images from six experiments) and (bottom) left hand somatosensory stimulation (averaged from seven experiments). Each column represents an image acquired every 25 s and consists of six transverse slices through the head arranged from the apex (top row) to a slice approximately through the visual cortex (bottom row). The images are orientated as if the subject is viewed from above (left diagram). The images are thresholded in order to show those changes that are more than 2 SE from baseline. Impedance decreases, probably due to increased regional cerebral blood volume, are seen in the approximate regions of the visual cortex (top) and contralateral somatosensory cortex (bottom), each with a similar time course to the stimulus. Significant impedance increases are also seen in red, these may be due to reconstruction artefact or impedance increases within the head.

likely that electrode placement errors accounted for the localization error in the human images.

The simplified reconstruction model may account for localization error, as the model does not contain information about the geometry of the human head, nor the different conductivities of the tissue layers that comprise the head, such as the scalp, skull, dura, CSF, and grey and white matter. In addition, the spherical model is symmetrical in all radial directions to current flow, whereas the head is anisotropic, i.e., it has different properties dependent on the direction of current flow (Joy *et al.,* 1999). These differences between the head and the reconstruction model may give rise to impedance changes being imaged remotely to their true position. In order to test this, we attempted to model some of the properties of the head, such as the irregular geometry and presence of the skull, in a head-shaped tank. Images from the tank demonstrate little localization error, although the presence of the skull caused a slight image distortion (Tidswell *et al.,* 2000), by which objects at the periphery of the skull were imaged more centrally by up to 5–10% of the image diameter. Although this distortion may have contributed to localisation error, it would not have been large enough to cause an inappropriate localization of an impedance change. However, there were limitations of

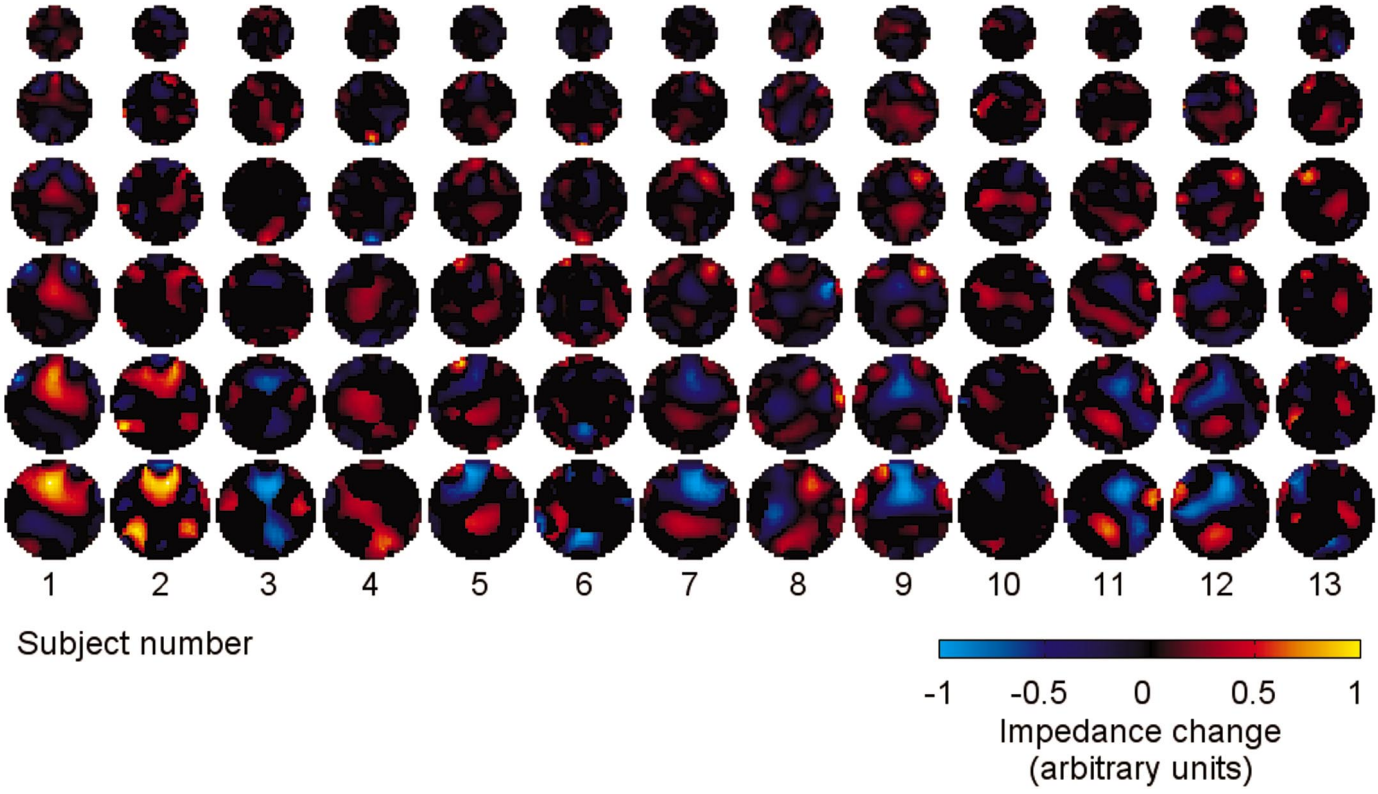

FIG. 5. Images during visual stimulation in 13 subjects (average of between 5–12 images per subject). The images are thresholded so that only impedance changes greater than 2 SE from the baseline are visible. Impedance changes are seen in the approximate area of the visual cortex in nine subjects. Both impedance increases and decreases are seen. There is a wide variation between subjects on the size and localization of the impedance changes seen. This variation may be due to a combination of either low signal or reconstruction artefacts or physiological impedance changes in areas outside the visual cortex.

the tank studies as neither tissue anisotropy, nor the different conductivities of the tissue layers of the head were simulated. Although the skull is the largest conductivity difference between the head and the reconstruction model, yet with a small effect on localization, it is still possible that smaller variations in conductivity due to tissue anisotropy and conductivity layers account for the large localization errors seen in the human images.

Additional localization errors may have been caused by reconstruction artefact, produced from the reconstruction algorithm, as these were present in the calibration images in the head-shaped tank (Fig. 2). The images demonstrated an appropriately localized impedance change that corresponded to the position of the sponge, but there were some smaller artefactual changes elsewhere which were of opposite polarity. These artefacts in the tank were small and it is unclear to what extent they contributed to localisation errors in the human images. It seems unlikely that they were the sole cause of these errors.

There may also have been a localization error due to temporal blurring of the impedance response in the images. Each image was acquired over 25 s. This was

TABLE 2

Stimulus-Related Impedance Changes Seen in the EIT Images during Human-Evoked Responses

Stimulation paradigm (number of subjects)	Images with significant change in the correct area	Images with significant change elsewhere	Images with no change
Visual (n = 13)	9 (5 decreases)	4 (4 decreases)	0
Motor (n = 20)	8 (4 decreases)	9 (8 decreases)	3
Somatosensory (n = 18)	2 (1 decrease)	5 (1 decrease)	11

Note. The number of images that had either a significant change or no change are indicated for each stimulation paradigm. The number of changes that were impedance decreases, the change expected from an increase in rCBV during stimulation, are indicated in brackets.

because the EIT system was based on the Hewlett-Packard HP 4284A analyzer, which uses a relatively slow but highly accurate bridge balancing system, and so this image time was unavoidable. The timecourse of the impedance change had a latency of 6 s after the start of stimulation, determined by individual inspection of the raw data. Measurements acquired early on in an image set, within the latency period, demonstrated no impedance change compared to measurements acquired after this period. It is therefore likely that this caused a temporal blurring of the impedance change in the initial image after stimulation. However, this is unlikely to have caused any significant degradation to image quality, as the localization of impedance changes were determined from the later stimulus images, acquired during a plateau phase of the impedance response.

An alternative explanation is that the EIT images represent the true impedance change within the human brain, confounded by small artefacts introduced by the reconstruction algorithm and measurement noise. As reconstruction artefacts and image noise are small in the tank calibration studies, then these are unlikely to be the main cause of the significant impedance changes in the human images. These significant changes are likely to be produced by either impedance increases or decreases within the activated cortex, or elsewhere in the brain. EIT images from rabbits suggests that only decreases in impedance occur during functional activity due to increased rCBV (Holder *et al.*, 1996). This is the likely cause of the impedance decreases seen in the human images, but this does not explain the presence of impedance increases. Physiological mechanisms which would cause cortical impedance to increase are either decreases of rCBV or neuronal and glial cell swelling. Animal evidence indicates that neuronal cells swell as a result of the ionic shifts, which accompany repetitive neuronal activity either in the axon (Cohen *et al.*, 1972) or in the cortex during epilepsy or electrical stimulation (Lux *et al.*, 1986; Andrew and Mac Vicar, 1994); this reduces the size of the low impedance extra-cellular space and increases impedance. As repetitive neuronal activity is also produced during functional activation paradigms, a lesser degree of cortical cell swelling may occur. The overall impedance measured would then be the sum of the opposing impedance changes due to cell swelling and increased rCBV, so we would not necessarily expect to see impedance decreases in all subjects. Although this may explain the presence of significant impedance increases, it does not account for the failure to localise these changes to the expected area in the image corresponding to the stimulated cortex.

This failure of localization might be explained, physiologically, by human studies in which the evoked rCBF response in stimulated cortex has been accompanied by areas of decreased rCBF in other regions of brain: this has been imaged optically over the motor cortex during motor activity (Haglund *et al.*, 1992) and frontal cortical areas by PET during visual evoked responses (Mentis *et al.*, 1997). Also, the area of rCBF increase is not limited to the primary motor or sensory cortex stimulated: ipsilateral as well as contralateral rCBF increases have been detected during unilateral hand motor activity (Kim *et al.*, 1993; Sadato *et al.*, 1996) and more widespread changes detected with PET during simple and complex sequential finger movements (Catalan *et al.*, 1998). These studies, with stimuli similar to the paradigms used in this study, indicate that the patterns of human cortical impedance changes may be complex; there are likely to be multiple impedance changes due to cell swelling, increased rCBV and decreased rCBV within and away from the functionally stimulated cortex. Due to the low resolution of EIT, these multiple changes might not be independently localized, so the EIT images represent a combination of multiple changes. As changes outside the stimulated cortex vary between subjects (Mentis, personal communication), then this would result in a variation of impedance change localisation between subjects, some of which would be incorrectly localised. This variation would seem to limit the use of EIT for functional imaging of the human brain. However, there is room for optimism: EIT of evoked responses is in its infancy, impedance changes could be measured in nearly all subjects during an evoked response task and over a third of these experiments demonstrated impedance changes near the expected site of stimulation. We are currently in the process of testing a faster EIT system which will allow more measurements to be made per image and we are introducing a realistic finite element head model into the reconstruction process. The aim of this model is to incorporate realistic geometric, conductivity, and, eventually, anisotropic information into the reconstruction process. We expect that these developments will improve image quality and allow multiple impedance changes to be resolved which would improve the use of EIT in neuroimaging.

In conclusion, we have presented the first work to demonstrate that impedance changes, associated with evoked response paradigms, can be measured non-invasively from the human head. Imaging of these responses is still at an early phase of development, but if the problems of low resolution and reconstruction error can be overcome then EIT could be used as a portable and fast neuroimaging tool with clinical applications in the imaging of epilepsy, migraine, and stroke.

REFERENCES

Adey, W., Kado, R., and Didio, J. 1962. Impedance measurements in brain tissue of animals using microvolt signals. *Exp. Neurol.* **5:** 47–66.

Aladjolova, N. A. 1964. Slow electrical processes in the brain. In *Progress in Brain Research,* Vol. 7, pp. 155–237.

Andrew, R., and Mac Vicar, B. 1994. Imaging cell volume changes and neuronal excitation in the hippocampal slice. *Neuroscience* **62**(2): 371–383.

Avis, N. J., Barber, D., Brown, B., and Kiber, M. 1992. Back-projection distortions in applied potential tomography images due to nonuniform reference conductivity distributions. *Clin. Phys. Physiol. Measur.* **13**(Suppl. A): 113–117.

Bayford, R. H., Boone, K. G., Hanquan, Y., and Holder, D. S. 1996. Improvement of the positional accuracy of EIT images of the head using a Language multiplier reconstruction algorithm with diametric excitation. *Physiol. Measure.* **17:** A49–A57.

Belliveau, J. W., Kennedy, D. N., McKinstry, R. C., Buchbinder, B. R., Weisskopf, R. M., Cohen, M. S., Vevea, J. M., Brady, T. J., and Rosen, B. R. 1991. Functional mapping of the Human Visual Cortex by Magnetic Resonance Imaging. *Science* **254:** 716–719.

Binnie, C., Rowan, A., and Gutter, T. 1982. The 10–20 system. In *A Manual of Electroencephalographic Technology,* pp. 325–331. Cambridge Univ. Press.

Boone, K., Lewis, A. M., and Holder, D. S. 1994. Imaging of cortical spreading depression by EIT: Implications for localization of epileptic foci. *Physiol. Measure.* **15:** A189–A198.

Boone, K., and Holder, D. 1995. Assessment of noise and drift artefacts in electrical impedance tomography measurements using the Sheffield Mark I system. *Innovat. Technol. Biol. Med.* **16**(S2): 49–60.

Breckon, W. 1990. Image reconstruction in electrical impedance tomography. *School of Computing and Mathematical Sciences,* PhD. Oxford Polytechnic.

Brown, B., and Seagar, A. 1987. The Sheffield data collection system. *Clin. Phys. Physiol. Measure.* **8**(A): 91–97.

Catalan, M. J., Honda, M., Weeks, R. A., Cohen, L. G., and Hallett, M. 1998. The functional neuroanatomy of simple and complex sequential finger movements: A PET study. *Brain* **121:** 253–264.

Cohen, L. B., Keynes, R. D., and Landowne, D. 1972. Changes in axon light scattering that accompany the action potential: Current-dependent components. *J. Neurophysiol.* **224:** 727–752.

Fox, P. T., Mintun, M. A., Raichle, M. E., Miezin, F. M., Allman, J. M., and Essen, D. C. V. 1986. Mapping visual cortex with positron emission tomography. *Nature* **323:** 806–809.

Geddes, L. A., and Baker, L. E. 1967. The specific resistance of biological material: A compendium of data for the biomedical engineer and physiologist. *Med. Biol. Eng.* **5:** 271–293.

Gersing, E. 1991. Messung der elektischen Impedanz von Organen-Apparative Ausrustung fur Forschung und klinische Anwendung. *Biomed. Technik* **36:** 6–11.

Gibson, A., Bayford, R., and Holder, D. 2000. Two-dimensional finite element modelling of the neonatal head. *Physiol. Measure.* **21:** 45–52.

Gibson, A. 2000. *Electrical Impedance Tomography of Human Brain Function,* PhD. Univ. College London, London.

Golub, G., and Loan, C. V. 1996. *Matrix Computations,* John Hopkins Univ. Press.

Haglund, M., Ojeman, G., and Hochman, D. 1992. Optical imaging of epileptiform and functional activity in human cerebral cortex. *Nature* **358:** 668–671.

Holder, D. S. 1992. Detection of cerebral ischaemia in the anaesthetised rat by impedance measurement with scalp electrodes: Implications for non-invasive imaging of stroke by electrical impedance tomography. *Clin. Phys. Physiol. Measure.* **13**(1): 63–75.

Holder, D., Boone, K., and Cusick, G. 1994. Specification for an electrical impedance tomogram for imaging epilepsy in ambulatory human subjects. *Innivat. Technol. Biol. Med.* **15**(S1): 24–32.

Holder, D. S., Rao, A., and Hanquan, Y. 1996. Imaging of physiologically evoked responses by electrical impedance tomography with cortical electrodes in the anaesthetised rabbit. *Physiol. Measure.* **17:** A179–A186.

Ibanez, V., Deiber, M. P., Sadato, N., Toro, C., Grissom, J., Woods, R. P., Mazziotta, J. C., and Hallett, M. 1995. Effects of stimulus rate on regional cerebral blood flow after median nerve stimulation. *Brain* **118:** 1339–1351.

Joy, M., Lebedeev, V., and Gati, J. 1999. Imaging of current density and current pathways in rabbit brain during transcranial electrostimulation. *IEEE Trans. Biomed. Eng.* **46**(9): 1139–1148.

Kim, S., Ashe, J., Georgopoulos, A., Merkle, H., Ellermann, J., Menon, R., Ogawa, S., and Ugurbil, K. 1993. Functional imaging of human motor cortex at high magnetic field. *J. Neurophysiol.* **69**(1).

Kinahan, P., and Noll, D. 1999. A direct comparison between whole-brain PET and BOLD fMRI measurements of single-subject activation response. *Neuroimage* **9:** 430–438.

Kwong, K. K., Belliveau, J. W., Chesler, D. A., Goldberg, I. E., Weisskopf, R. M., Poncelet, B. P., Kennedy, D. N., Hoppel, B. E., Cohen, M. S., Turner, R., Cheng, H., Brady, T. J., and Rosen, B. R. 1992. Dynamic magnetic resonance imaging of the human brain activity during primary sensory stimulation. *Proc. Natl. Acad. Sci. USA* **89:** 5675–5679.

Lux, H., Heinemann, U., and Dietzel, I. 1986. Ionic changes and alterations in the size of the extracellular space during epileptic activity. In *Advances in Neurology* (A. Delgado-Escueta, A., Ward, D., Woodbury, and R. Porter, Ed.), Vol. 44.

Malonek, D., Dirnagl, U., Lindauer, U., Yamada, K., Kanno, I., and Grinvald, A. 1997. Vascular imprints of neuronal activity: Relationships between the dynamics of cortical blood flow, oxygenation and volume changes following sensory stimulation. *Proc. Natl. Acad. Sci. USA* **94:** 14826–14831.

Mangall, Y., Baxter, A., Avill, R., Bird, N., Brown, B., Barber, D., Seager, A., Johnson, A., and Read, N. 1987. Applied Potential Tomography: A new noninvasive technique for assessing gastric function. *Clin. Phys. Physiol. Measure.* **8**(A): 119–129.

Mazziotta, J. C., and Phelps, M. 1984. Human sensory stimulation and deprivation: Positron Emission Tomographic results and strategies. *Ann. Neurol. (Suppl.)* **15:** S50–S60.

Mentis, M. J., Alexander, G. E., Grady, C. L., Horowitz, B., Krasuski, J., Pietrini, P., Strassburger, T., Hampel, H., Schapiro, M. B., and Rappoport, S. I. 1997. Frequency variation of a pattern-flash visual stimulus during PET differentially activates brain from striate through frontal cortex. *Neuroimage* **5:** 116–128.

Metherall, P., Barber, D. C., Smallwood, R. H., and Brown, B. H. 1996. Three-dimensional electrical impedance tomography. *Nature* **380:** 509–512.

Palmer, J., de-Crespigny, A., Williams, S., Busch, E., and van-Bruggen, N. 1999. High Resolution mapping of discrete representational areas in rat somatosensory cortex using blood volume dependent functional MRI. *Neuroimage* **9:** 383–392.

Ranck, J. B. 1963. Specific impedance of rabbit cerebral cortex. *Exp. Neurol.* **7:** 144–152.

Rao, A. 2000. *Electrical Impedance Tomography of Brain Activity: Studies into Its Accuracy and Physiological Mechanisms*, Ph.D. Univ. College London, London.

Sadato, N., Campbell, G., Ibanez, V., Deiber, M., and Hallett, M. 1996. Complexity affects regional cerebral blood flow during sequential finger movements. *J. Neurosci.* **16**(8): 2693–2700.

Tarassenko, L., Pidcock, M., Murphy, D., and Rolfe, P. 1985. The development of impedance imaging techniques for use in the newborn at risk of intra-ventricular haemorrhage *IEEE Int. Conf. Electric Magn. Fields Med. Biol.* 83–87.

Tidswell, A., Gibson, A., Bayford, R., and Holder, D. 2000. Validation of a 3-D reconstruction algorithm for EIT of human brain function in a realistic head shaped tank. *In press.*

Van-Harreveld, A., and Ochs, S. 1956. Cerebral Impedance Changes after circulatory arrest. *Am. J. Physiol.* **187:** 180–192.

Van-Harreveld, A., and Schade, J. 1962. Changes in the electrical conductivity of cerebral cortex during seizure activity. *Exp. Neurol.* **5:** 383–400.

Yablonskiy, D., Ackerman, J., and Raichle, M. 2000. Coupling between changes in human brain temperature and oxidative metabolism during prolonged visual stimulation. *Proc. N.Y. Acad. Sci.* **97**(13): 7603–7608.